

adequate delineation of the abnormalities was more difficult than with  $^{111}\text{In}$ -leukocytes or  $^{111}\text{In}$ -liposomes.

## ACKNOWLEDGMENTS

We thank Mr. G. Grutters and Mr. H. Eikholt (Central Animal Laboratory, University of Nijmegen, The Netherlands) for their help in performing the study. The study was supported by a grant from the Foundation of Technical Sciences (Stichting voor de Technische Wetenschappen, STW), The Netherlands. The polyethylene glycol 1900 derivative of distearoyl phosphatidylethanolamine was a gift from Liposome Technology, Inc. (Menlo Park, CA). Cholesterol was from Sigma Chemical Co. (St. Louis, MO) and glutathione from E. Merck (Darmstadt, Germany).

## REFERENCES

1. Crama-Bohouth GE, Pena AS, Arndt JW, et al. Value of indium-111 tropolonate autologous granulocyte scintigraphy in the assessment of inflammatory bowel disease. *Scand J Gastroenterol* 1990;178(suppl):93-98.
2. Lange JMA, Boucher CAB, Hollak CEM, et al. Failure of zidovudine prophylaxis after accidental exposure to HIV-1. *N Engl J Med* 1990;322:1375-1377.
3. Rojas-Burk J. Health officials reactions to infection mishaps. *J Nucl Med* 1992;33:13N-27N.
4. Oyen WJG, Claessens RAMJ, van der Meer JWM, Corstens FHM. Detection of subacute infectious foci with indium-111-labeled autologous leukocytes and with indium-111-labeled human nonspecific immunoglobulin G: a prospective comparative study. *J Nucl Med* 1991;32:1854-1860.
5. Oyen WJG, Claessens RAMJ, van der Meer JWM, Rubin RH, Strauss HW, Corstens FHM. Indium-111-labeled human nonspecific immunoglobulin G: a new radiopharmaceutical for imaging infectious and inflammatory foci. *Clin Infect Dis* 1992;14:1110-1119.
6. Morgan JR, Williams LA, Howard CB. Technetium-labeled liposome imaging for deep-seated infection. *Br J Radiol* 1985;58:35-39.
7. O'Sullivan MM, Powell N, French AP, Williams KE, Morgan JR, Williams BD. Inflammatory joint disease: a comparison of liposome scanning, bone scanning and radiography. *Ann Rheum Dis* 1988;47:485-491.
8. Karlowsky JA, Zhanel GG. Concepts on the use of liposomal antimicrobial agents: applications for aminoglycosides. *Clin Infect Dis* 1992;15:654-667.
9. Boerman OC, Storm G, Oyen WJG, et al. Sterically stabilized liposomes labeled with indium-111 to image focal infection. *J Nucl Med* 1995;35:1639-1644.
10. Bakker-Woudenberg IAJM, Lokerse AF, ten Kate MT, Mouton JW, Woodle MC, Storm G. Liposomes with prolonged blood circulation and selective localization in *Klebsiella pneumoniae*-infected lung tissue. *J Infect Dis* 1993;168:164-171.
11. Storm G, Belliot SO, Daemen T, Lasic DD. Surface modification of nanoparticles to oppose uptake by the mononuclear phagocyte system. *Adv Drug Delivery Res* 1995;17:31-48.
12. Allgayer H, Deschryver K, Stenson WF. Treatment with 16,16'-dimethyl prostaglandin  $\text{E}_2$  before and after induction of colitis with trinitrobenzenesulfonic acid in rats decreases inflammation. *Gastroenterology* 1989;96:1290-1300.
13. Percy WH, Buron MB, Rose K, Donovan V, Burakoff R. In vitro changes in the properties of rabbit colonic muscularis mucosae in colitis. *Gastroenterology* 1993;104:369-376.
14. Kim HS, Berstad A. Experimental colitis in animal models. *Scand J Gastroenterol* 1992;27:529-537.
15. Babich JW, Graham W, Barrow SA, et al. Technetium-99m-labeled chemotactic peptides: comparison with indium-111-labeled white blood cells for localizing acute bacterial infection in the rabbit. *J Nucl Med* 1993;34:2176-2181.
16. Oyen WJG, Boerman OC, Storm G, et al. Labeled stealth liposomes in experimental infection: an alternative for leukocyte scintigraphy? *Nucl Med Commun* 1996;17:742-748.
17. Lang J, Vigo-Pelfrey C, Martin F. Liposomes composed of partially hydrogenated egg phosphatidylcholines: fatty acid composition, thermal phase behavior and oxidative stability. *Chem Phys Lipids* 1990;53:91-101.
18. Woodle MC, Mathay KK, Newman MS, et al. Versatility in lipid compositions showing prolonged circulation with sterically stabilized liposomes. *Biochim Biophys Acta* 1992;1105:193-200.
19. Storm G, van Bloois L, Brouwer M, Crommelin DJA. The interaction of cytostatic drugs with adsorbents in aqueous media. The potential implication for liposome preparation. *Biochim Biophys Acta* 1985;818:343-351.
20. Gabizon A, Huberty, Straubinger RM, Price DC, Papahadjopoulos D. An improved method for in vivo tracing and imaging of liposomes using a gallium 67-deferoxamine complex. *J Liposome Res* 1988;1:123-135.
21. Hnatowich DJ, Childs RL, Lanteigne D, Najafi A. The preparation of DTPA-coupled antibodies radiolabeled with metallic radionuclides: an improved method. *J Immunol Methods* 1983;65:147-157.
22. Lantto E, Jarvi K, Krekela I, Lantto T, Taavitsainen M, Vedenkangas H, Vorne M. Technetium-99m-hexamethylpropylene amine oxine leukocytes in the assessment of disease activity in inflammatory bowel disease. *Eur J Nucl Med* 1992;19:14-18.
23. Thakur ML, McAfee JG. The significance of chromosomal aberrations in indium-111-labeled lymphocytes. *J Nucl Med* 1984;25:922-927.
24. Arndt JW, van der Sluys-Veer A, Blok D, et al. A prospective comparison of technetium-99m-labeled polyclonal human immunoglobulin and indium-111 granulocytes for localization of inflammatory bowel disease. *Acta Radiol* 1992;33:140-144.
25. Oyen WJG, Naber AHJ, Claessens RAMJ, van der Meer JWM, Corstens FHM. Evaluation of inflammatory bowel disease activity with indium-111-labeled human nonspecific immunoglobulin G [Abstract]. *J Nucl Med* 1992;33:919.
26. Oyen WJG, Boerman OC, van der Laken CJ, Claessens RAMJ, van der Meer JWM, Corstens FHM. The uptake mechanisms of inflammation and infection localizing agents. *Eur J Nucl Med* 1996;23:459-465.
27. Saverymuttu SH, Peters AM, Danpure HJ, Reavy HJ, Osman S, Lavender JP. Lung transit of indium-111-labeled granulocytes: relationship to labeling techniques. *Scand J Haematol* 1983;30:151-160.
28. Wheeler JG, Slack NF, Duncan A, Palmer M, Harvey RF. Technetium-99m-nanocolloid imaging in inflammatory bowel disease. *Nucl Med Commun* 1990;11:127-133.
29. Arndt JW, van der Sluys-Veer A, Blok D, et al. Technetium-99m-nanocolloid for the scintigraphic assessment of inflammatory bowel disease in the colon: its value in comparison with indium-111-labeled granulocytes. *Eur J Radiol* 1991;12:30-34.

# Improved Wrist Fracture Localization with Digital Overlay of Bone Scintigrams and Radiographs

W. Roolker, M.M.C. Tiel-van Buul, A.H. Broekhuizen, A.K. Eikelenboom and E.A. van Royen

Departments of Nuclear Medicine, Surgery and Radiology, Academic Medical Center, Amsterdam, The Netherlands

The diagnosis of scaphoid fracture is often difficult and of interest in traumatology. Because of the low sensitivity of repeated scaphoid radiographs, a bone scintigram is advocated and considered the gold standard. In this study, we tried to simplify the interpretation of the bone scintigram of hand and wrist in localizing the hot spot by the digital overlay of the radiograph and the bone scintigram, using a simple device, in patients after wrist trauma. **Methods:** Twenty-one consecutive patients (22 wrists) with clinically-suspected scaphoid fracture and negative initial radiographs were included. The PA view of the wrist was obtained with the hand of the patient placed in an acrylic device with three lead markers. For the bone scan, a similar device was used with  $^{57}\text{Co}$  markers at the same

positions. We called this device the "hand-fix." The PA radiograph was digitized with a videocamera and overlaid on the bone scan. Each bone scan was interpreted twice by each of three observers, one nuclear physician and two residents in nuclear medicine. The first interpretation was made without the digital overlay, and the second was made with the digital overlay. **Results:** The bone scintigrams were positive in the scaphoid, distal radius and in other carpal bones. Out of the 22 bone scans, Observer 1 judged 19 correctly, Observer 2 judged 16 correctly and Observer 3 judged 10 correctly without the digital overlay images. All three observers gave a correct localization in the 22 wrists using the digital overlay images. **Conclusion:** The digital overlay of a radiograph and a bone scintigram, using the hand-fix, simplifies and improves interpreting and localizing the hot spot on bone scintigrams in patients with wrist injuries.

**Key Words:** wrist; bone scintigraphy; multimodality

**J Nucl Med** 1997; 38:1600-1603

Received Aug. 1, 1996; revision accepted Nov. 6, 1996.

For correspondence or reprints contact: W. Roolker, MD, Department of Nuclear Medicine, F2Noord, Academic Medical Center, Meibergdreef 9, 1105 AZ Amsterdam, The Netherlands.

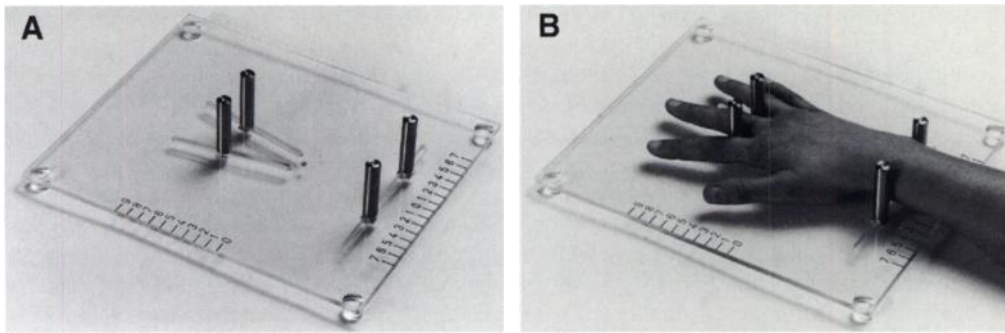


**FIGURE 1.** (A) The hand-fix device for obtaining the radiographs with three lead markers. (B) Positioning the wrist in the hand fix.

**D**ifficulty in interpreting radiographs after carpal injury emphasizes the importance of clinical assessment in diagnosing scaphoid fractures. Initial scaphoid radiographs have a sensitivity of 64% and are noninvasive, inexpensive and provide adequate anatomical information. These radiographs are diagnostically reliable in patients in whom a fracture can be identified (1). Alternatively, a radionuclide bone scintigram performed after 72 hr following injury is a highly sensitive,

noninvasive technique and, if negative, essentially excludes an acute fracture in a patient (2,3). The bone scan is well accepted in the further investigation of patients after wrist trauma. Although the specificity of the bone scan is high (98%) in the diagnosis of scaphoid fracture, the exact localization of the hot spot in the carpus often is difficult to interpret and sometimes makes an accurate diagnosis impossible (4). The high specificity found in this previous study was reached in an academic

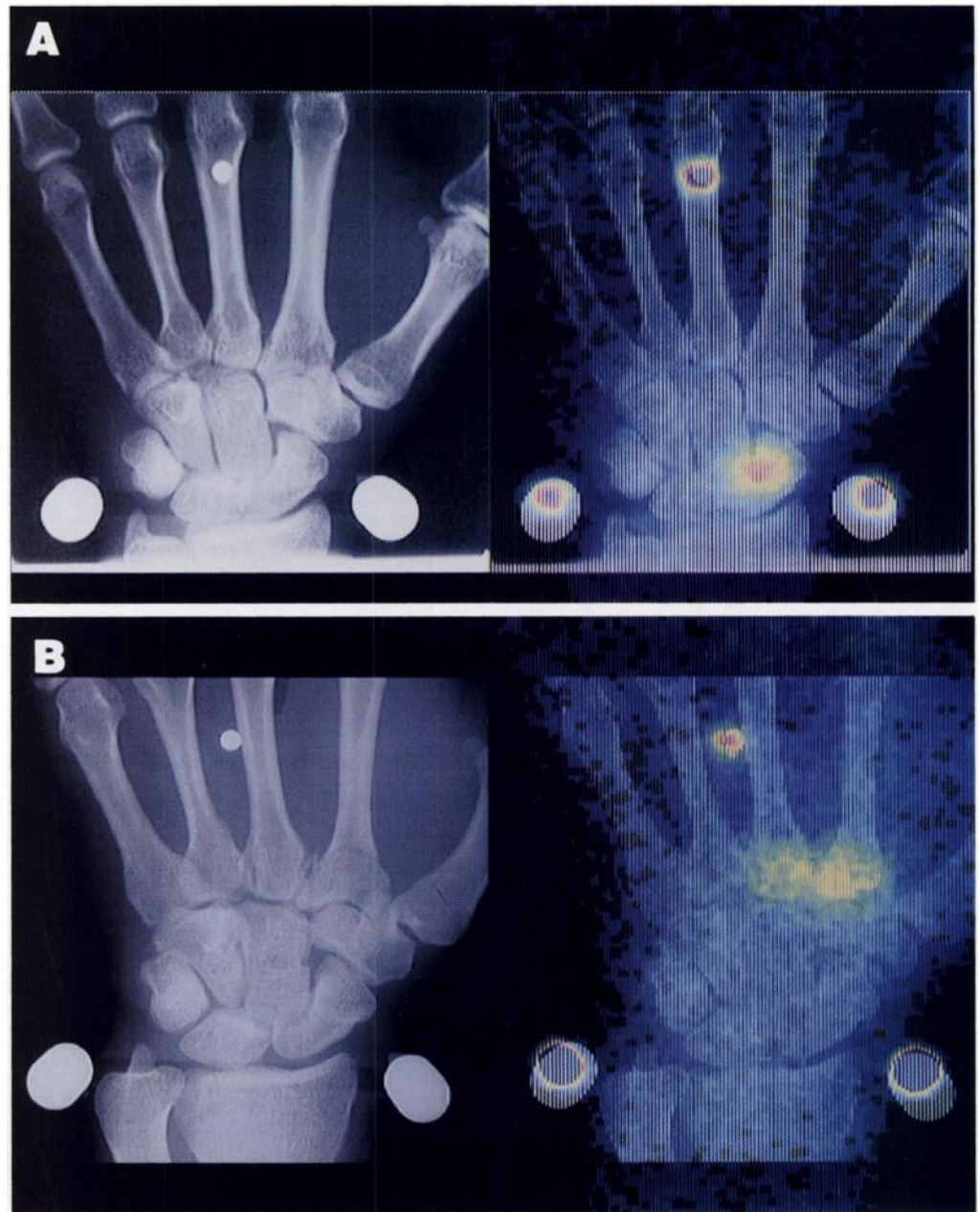


**FIGURE 2.** (A) Digital overlay of the radiograph over the bone scan in a patient with a proven scaphoid fracture on the radiograph. (B) Digital overlay of the radiograph over the bone scan in a patient with a fracture of the proximal metacarpals II and III.

setting with special interest for the diagnostic management of scaphoid fracture. It can be questioned if the same specificity would be found in a general nuclear medicine practice.

During the last few years, alternative imaging modalities have increased. The information acquired with the various imaging modalities makes it possible to exploit the potential of two or more combined modalities to obtain additional, accurate information.

Nuclear medicine images generally have poor spatial resolution, making it difficult to relate the functional information that they contain to precise anatomical structures. Combining images from nuclear medicine and the anatomical information from CT and MRI has been widely reported in studies of the brain and heart (5-7). This type of multimodality imaging consists of geometric registration, data combination and interpretation of the images. Clinical applications of the integration of multimodality imaging require efficient and fast data transfer, standardization of procedures and implementation of techniques for the registration. Henze et al. (8) reported a protocol for defining projections of SPECT data that correspond to the dental orthopan radiograph. When comparing SPECT data with radiograph images, they were able to reduce the three-dimensional registration to two dimensions. In our application, the projection of the bone scan and the radiograph are identical to reduce the registration in two dimensions (8).

In this study, we attempted to simplify the interpretation of the bone scan in localizing the carpal hot spot by digital overlay of the PA radiograph and the PA bone scan using a new device that we called the "hand-fix."

## MATERIALS AND METHODS

In this study, 21 consecutive patients (22 wrists), 11 men and 10 women, mean age 43 yr (range 17-64 yr) with a history of a wrist trauma who were clinically suspected for scaphoid fracture were included. The radiographs of these 21 patients were all read as negative.

### Radiograph Acquisition

Scaphoid radiographs in four directions were obtained routinely. If they were positive, the patient was treated. If they were negative or dubious, an additional radiograph of the injured wrist was obtained with the hand placed on an acrylic phantom (the hand-fix). All the patients who were included were taken by one investigator to the department of radiology. The patients were asked to place their hand in the acrylic device with the middle finger between two lead bars and the distal radius and ulna between two other lead bars. The forearm was in a direct line with metacarpal III, with the wrist in a neutral position. Three markers on the acrylic device were used for registration. One of the markers was at the distal part of metacarpal III, while the other two markers were beside the distal radius and ulna (Fig. 1 A, B). A PA radiograph was taken of the wrist with the camera tube placed 95 cm away. The radiograph included the metacarpo-phalanx and the distal radius and ulna. The investigator registered the marker's position. After the radiograph was obtained, it was placed on a lightbox and digitized with a Canon UC-X1 Hi videocamera (Canon Inc., Tokyo, Japan), using a computer program on a UNIX operating system to convert it into Interfile format. The image was recorded in a 512 × 512 format and stored on the UNIX machine.

### Bone Scintigram

A three-phase bone scintigram was obtained three to six days after trauma, using 200 MBq <sup>99m</sup>Tc-methyldiphosphonate. Images were acquired on a Siemens Diacam gamma camera (Siemens, Hauge, The Netherlands) with a parallel-hole, high-resolution collimator and interfaced to a Hermes® acquisition system (Nuclear Diagnostics AB, Hagestren, Sweden). Dynamic blood flow

images were acquired for 60 sec, and a single diffusion image was obtained for 5 min, corresponding to the primary blood pool. Two hours after injection, anterior and lateral static views were obtained in a preset time of 5 min. The bone scan was considered positive if focally increased activity (a hot spot) was seen in the scaphoid region both at the dynamic and static images. A hot spot in both images in another carpal region was judged as another fracture.

After the routine bone scan images, one image (256 × 256) was obtained from the injured wrist. The patients placed their wrist in the acrylic device, with three markers of <sup>57</sup>Co, in the same position for the radiograph and performed by the same investigator. This image also was obtained on the Siemens Diacam gamma camera, using 1.75 magnification with a 5-min duration. The image was stored on the UNIX system.

Both images were selected on the UNIX computer, using a commercial multimodality image program (Multimodality program, Hermes® package, Nuclear Diagnostics) (9). Both the radiograph and bone scan images were adjusted for differences in size and automatically registered. Both images were overlaid after this procedure.

All the bone scans were blind and independently judged by one nuclear physician and two residents in nuclear medicine. None of the physicians had knowledge of the result of the digital overlay of the radiographs over the bone scan. The bone scan was judged correctly if the interpreted localization was identical with the localization of the hot spot found by the overlay technique. To compare the results of the three observers, we used the Student's t-test for statistical analysis.

## RESULTS

In all 21 patients the bone scintigram showed a hot spot in the carpus, nine showed hot spots in the scaphoid region, seven in the distal radius and six elsewhere in the carpus/hand. In one female patient both wrists were affected, one in the scaphoid region and one in the distal radius. In two patients, a scaphoid fracture was retrospectively recognized on the initial radiographs, both with a hot spot in the scaphoid region on the bone scan. In one other patient, fractures of the proximal MCP II and III were initially recognized, also with clinical suspicion of a scaphoid fracture and, therefore, referred for a bone scan. In this patient, the bone scan showed only hot spots in the known MCP fractures but remained negative in the region of the scaphoid. The overlay technique in these three patients proved that the hot spot was at the same place as where the fractures were recognized (Fig. 2 A,B).

Observer 1 judged 19 of 22 affected wrists on the bone scan correctly, Observer 2 judged 16 correctly and Observer 3 judged 10 correctly. There was a significant difference in judgement between Observers 1 and 3 ( $p < 0.01$ ) and between Observers 2 and 3 ( $p < 0.04$ ). After the initial judgements, the three observers were asked to judge the digital overlay images. All three observers were now able to give an exact localization of the hot spot seen on the bone scan in the 22 affected wrists using the digital overlay technique.

Table 1 summarizes the results of the 22 cases evaluated by the three observers. None of the bone scans was judged as normal. For the first observer, the digital overlay images improved the localization in three of 22 scans. For the second observer, the localization was improved in six of 22 scans, while for the third observer localization was improved in 12 of 22 scans. All three observers agreed that the digital overlay images improved the interpretation of the localization of the hot spots seen in the wrists. Also, in those cases that were initially judged correctly, the digital overlay images were perceived by the observers as simplifying the interpretation of the bone scan.

**TABLE 1**  
Results of Assessment of Digital Overlay in 22 Wrists by  
Three Observers

| Observer | Abnormal without digital overlay | Abnormal with digital overlay | Improved localization |
|----------|----------------------------------|-------------------------------|-----------------------|
| 1        | 19                               | 22                            | 3                     |
| 2        | 16                               | 22                            | 6                     |
| 3        | 10                               | 22                            | 12                    |

## DISCUSSION

The evaluation of wrist pain, after trauma, is a common clinical problem. The sensitivity of bone scintigram is approximately 100%, and the specificity is found to be maximally 98% [95% C.I. 88%–100%], but sometimes it is difficult to give an exact localization of the hot spot seen on the bone scan, especially of the carpus. This was found in our academic institution with a specific interest in the diagnostic imaging of scaphoid fractures. The specificity is probably less in a general nuclear medicine department lacking special expertise in this area.

## CONCLUSION

In this study the digital overlay technique clearly improved the interpretation of the localization of the carpal hot spot, which may lead to a higher specificity of the bone scan. The hand-fix proved to be a simple acrylic device for matching the images. A multimodality program must be available for producing these overlaid images. Our results demonstrate that this application significantly improves the diagnostic effectiveness of routine bone scan imaging in hand and wrist injuries. However, the hand-fix device used in this study could be improved. The height of the marker cylinders induced a small

parallax error (seen in Fig. 2 A, B). This error can be reduced if the heights of the marker cylinders are reduced.

This technique, in which a videocamera was used to digitize the radiographs, can be further simplified if the acquisition of scaphoid series is also digital. In that case, a network connection between the radiology and nuclear medicine departments is required. Otherwise, a good quality film digitizer or videocamera and frame grabber board can be used.

## ACKNOWLEDGMENTS

We thank the nuclear medicine physician and the two residents for judging the bone scans and the technologists of the radiology department for their help.

## REFERENCES

1. Tiel-van Buul MMC, van Beek EJR, Broekhuizen AH, Nootgedacht EA, Davids PHP, Bakker AJ. Diagnosing scaphoid fractures: radiographs cannot be used as a gold standard. *Injury* 1992;23:77–79.
2. Shewring DJ, Savage R, Thomas G. Experience of the early use of technetium-99 bone scintigraphy in wrist injury. *J Hand Surg [Br]* 1994;19B:114–117.
3. Waizenegger M, Wastie ML, Barton NJ, Davis RC. Scintigraphy in the evaluation of the "clinical" scaphoid fracture. *Hand Surg [Br]* 1994;19B:6:750–753.
4. Tiel-van Buul MMC, van Beek EJR, Dijkstra PF, Bakker AJ, Broekhuizen AH, van Royen EA. Significance of a hot spot on the bone scan after carpal injury—evaluation by computed tomography. *Eur J Nucl Med* 1993;20:159–164.
5. Alpert NM, Bradshaw JF, Kennedy D, Correia JA. The principal axes information—a method for image registration. *J Nucl Med* 1990;31:1717–1722.
6. Lehmann ED, Hawkes DJ, Hill DLG, Bird CF, Robinson GP, Colchester ACF, Maisey MN. Computer-aided interpretation of SPECT images of the brain using an MRI-derived three-dimensional neuro-anatomical atlas. *Med Inform* 1991;16:151–166.
7. Slomka PJ, Hurwitz GA, Stephenson J, Craddock T. Automated alignment and sizing of myocardial stress and rest scans to three-dimensional normal templates using an image registration algorithm. *J Nucl Med* 1995;36:115–122.
8. Henze E, Graf G, Clausen M, et al. The orthopan tomoscintigram—a new application of emission computed tomography for facial bone scanning. *Eur J Nucl Med* 1990;16:97–101.
9. Slomka PJ, Hurwitz GA, Stephenson JA, et al. A volume-based image registration toolkit for automated comparison of paired nuclear medicine images [Abstract]. *Med Phys* 1995;22:1017.

# Internal Dose Estimation Including the Nasal Cavity and Major Airway for Continuous Inhalation of $C^{15}O_2$ , $^{15}O_2$ and $C^{15}O$ Using the Thermoluminescent Dosimeter Method

H.M. Deloar, H. Watabe, T. Nakamura, Y. Narita, A. Yamadera, T. Fujiwara and M. Itoh  
*Cyclotron and Radioisotope Center, Tohoku University, Aoba, Aramaki, Japan*

In the steady state method,  $^{15}O$ -labeled gases ( $C^{15}O_2$ ,  $^{15}O_2$  and  $C^{15}O$ ) are administered to the body by continuous inhalation in various clinical PET studies. During inhalation, the nasal cavity and major airway may obtain a substantial amount of dose, being the source organs as well as the target organs. The internal absorbed dose to those organs and their contribution to the other target organs have not been calculated by the MIRD method. To calculate the internal dose in the MIRD method, the S values, the absorbed doses per unit of cumulated activities from nasal cavity and major airway to the other organs and vice versa, are needed, and these values are not available. **Methods:** In this study, we introduced a

mathematical model of the nasal cavity and major airway to calculate their S values to 23 target organs and from 11 source organs to them. Individual experiments were performed to measure the total uptake percentage and body surface doses of  $^{15}O$ -labeled gases from continuous inhalation. **Results:** Using the body surface doses measured by thermoluminescent dosimeters, the cumulated activities of 11 source organs were estimated with the mathematical transformation method, and then the internal absorbed doses in 23 target organs were calculated by the MIRD method. Our experimental results were compared with the other results, and good agreements were observed. **Conclusion:** Among the target organs, the critical organ is the airway, and the absorbed dose is  $2.57 \times 10^{-2} \text{ mGy} \cdot \text{MBq}^{-1}$ .

**Key Words:** steady state technique; TLD; MIRD method;  $^{15}O$  inhalation; SAF

**J Nucl Med 1997; 38:1603–1613**

Received Jun. 3, 1996; accepted Nov. 6, 1996.  
For correspondence or reprints contact: Prof. T. Nakamura, Cyclotron and Radioisotope Center, Tohoku University, Aoba, Aramaki, Aoba-ku, Sendai-980, Japan.